David Tomás Sánchez Martínez
Lourdes García Rodríguez
(coordinadores)

# Proceedings of the 7th International Seminar on ORC Power Systems

Editorial Universidad de Sevilla

Proceedings of the 7th International Seminar on

# ORC
# Power Systems

David Tomás Sánchez Martínez
Lourdes García Rodríguez
(coordinadores)

Proceedings of the 7th International Seminar on

# ORC Power Systems

# (ORC2023)

4th to 6th
SEPTEMBER
SEVILLE 2023

EDITORIAL UNIVERSIDAD DE SEVILLA

Sevilla, 2024

Colección Actas
Núm.: 91



Review chairs of the 7th International Seminar on ORC Power Systems

Prof. Christoph Wieland (University of Duisburg-Essen) - *Review Chair*
Prof. Sotirios Karellas (National Technical University of Athens) - *Review Co-Chair*
Prof. Teemu Turunen-Saaresti (LUT University) - *Review Co-Chair*
Dr. Diego-César Alarcón-Padilla (Plataforma Solar de Almería - CIEMAT) - *Review Co-Chair*
Dr. Francesco Crespi (Universidad de Sevilla) - *Review Co-Chair*


c/ Porvenir, 27 - 41013 Sevilla.
Tlfs.: 954 487 447; 954 487 451; Fax: 954 487 443
Correo electrónico: info-eus@us.es
Web: https://editorial.us.es



ISBN 978-84-472-2745-7
DOI: https://dx.doi.org/10.12795/9788447227457

Diseño de cubierta y maquetación: los autores

## INDEX OF CONTRIBUTIONS

SEVILLE 2023
7th International Seminar on O.R.C. Power Systems

DOI: https://dx.doi.org/10.12795/9788447227457_141



# OPTIMUM COUPLING OF THERMAL ENERGY STORAGE AND POWER CYCLES FOR CARNOT BATTERIES

Salvatore Guccione[1,]*, Rafael Guedez[1]

[1] *KTH Royal Institute of Technology, Brinellvägen 68, 100 44, Stockholm, Sweden*

*Corresponding Author: guccione@kth.se

## ABSTRACT

To enable the widespread exploitation of intermittent, low-cost, and non-dispatchable renewable energy technologies, energy storage plays a key role in providing the required flexibility. In the spectrum of energy storage systems, one out of a few geographically independent possibilities is the storage of electricity into heat, so-called Carnot batteries. For thermal-to-electricity reconversion, depending on the operating energy storage temperatures, conventional or advanced power cycles can be integrated into the system, yielding different techno-economic performances. This work proposes a methodology that enables decision-making in selecting the adequate power cycle and Thermal Energy Storage (TES) type for a wide range of operating temperatures between 200 and 800 °C. To select the optimum coupling of TES and power block, a techno-economic optimization has been conducted aimed at minimizing the Levelized Cost of Storage (LCOS) for different plant capacities and charging costs. The study explores various power block configurations, including Organic Rankine Cycle (ORC), steam Rankine cycle, and supercritical $CO_2$ ($sCO_2$) Brayton cycle. Additionally, it evaluates different TES options such as molten salt, particle, and air packed bed TES. Results highlight that, for a charging cost of 50 EUR/MWh, the most cost-effective combination of TES and power block involves $sCO_2$ power blocks with recompression and intercooling, along with particle-based TES operating at temperatures between 600 to 800 °C and a temperature difference of 200 °C. ORCs are suitable for low temperatures (up to 350 °C) and high temperature differences, while the steam Rankine cycle is considered optimal between the low-temperature and the $sCO_2$ preferred regions. Air-packed bed TES is suggested as a viable option when TES represents a large share of the capital cost, with low charging costs, low hot temperatures, or low temperature differences. Molten salt TES is ideal when its design temperatures align with the operating limitations of the salts. Particle-based TES is the most cost-effective choice across a wide range of temperatures, at small (10 MW) and large scales (100 and 200 MW).



## 1 INTRODUCTION

To address the growing need for flexibility, cost-effectiveness, and efficiency in storing energy from fluctuating renewable sources, the utilization of energy storage systems has become crucial. Among the viable options, Carnot batteries have emerged as a cost-effective solution. During the charging phase, electricity is transformed into thermal energy and stored. Subsequently, during the discharging process, the stored heat is converted back into electricity. This approach enables the balancing of energy supply and demand while ensuring a reliable and secure energy supply (Benato & Stoppato, 2018). Previous studies have examined the technologies and configurations of Carnot batteries, along with performance metrics and experimental prototypes (Vecchi et al., 2022). Studies have examined technical barriers and selection criteria for key components of Carnot batteries for specific applications (Liang et al., 2022). At the system level, several techno-economic studies have been conducted to optimize both round-trip efficiency and financial metrics for two groups of Carnot batteries: Rankine-based (Hu et al., 2021) and Brayton-based (Albert et al., 2022). Rankine-based configurations include water steam Rankine cycles, trans-critical CO2 Rankine cycles (Morandin et al., 2012), and organic Rankine cycles (Frate et al., 2020). Brayton cycles with $sCO_2$ are considered a promising candidate due to their high thermal efficiency for heat sources above 350 °C, simple and compact physical footprint, and good operational flexibility to deal with uncertain renewable energy source availability (White et al., 2021). The potential of $sCO_2$ has been confirmed by the increase in research activity and international financial support for technological development over the last decade. Carnot batteries store energy using sensible heat, which can be in the form of liquids (Laughlin, 2017) or solid like molten salts and rocks. However, the working temperature range of molten salts is limited due to the high melting temperature of 240 °C and the chemical decomposition limit of 580 °C (D'Aguanno et al., 2018), making them challenging to use for high-temperature applications beyond 600 °C, and requiring costly maintenance. Particle-based thermal energy storage technology provides notable advantages over traditional systems, as it can maintain stability even at high temperatures up to 1200 °C, is resistant to corrosion, utilizes low-cost materials, and allows for cycle selection and optimization due to its broad temperature range (Ma, 2020). Packed bed systems store energy by heating and cooling solid particles through a heat transfer fluid that passes through the bed (Hänchen et al., 2011). Air is a promising heat transfer fluid due to its low cost, safety, availability, and direct heat transfer capabilities with the storage material. Alumina Energy has proposed a system that uses low-cost, high-temperature stable particles to store and recover thermal energy up to 1600 °C (Al-Azawii et al., 2021). Despite previous investigations into storage technologies and power cycles at the component and system levels for specific applications, a literature gap still exists in the form of a comprehensive study that compares the various combinations of these technologies. There is a lack of a comprehensive analysis to evaluate which power cycle represents the most cost-effective solution depending on the type of thermal energy storage and system boundary conditions, as noted by the authors. To fill the identified gap, the present study proposes a methodology that enables decision-making for the selection of an appropriate power cycle and TES for a range of operating temperatures that include heat sources from 200 to 800 °C. This study investigates a broad spectrum of power block configurations, including organic Rankine, steam Rankine, and supercritical $CO_2$, ($sCO_2$) Bryton cycles. A techno-economic optimization has been conducted to determine the optimum coupling of power cycles and TES technology, including molten salt, particle, and air packed bed TES. In developing quasi-steady state system models, the study considers variable boundary conditions, scale-dependent cost functions, performance correlations, different heat sources and maximum temperature difference that is compatible with various storage technologies. The study investigates the impact of scale and charging cost on the performance of the system through sensitivity analyses.

## 2 SYSTEM DESCRIPTION

Figure 1 shows the schematic of the introduced energy storage plant. The system uses an electric heater to convert electricity sourced from either the electric grid or a renewable electricity system into thermal energy, which is then stored in the TES. A power block is integrated into the system to enable thermal-to-electricity reconversion. During periods of low-cost electricity or intermittent renewable electricity production, the Electric Heater (EH) is used to charge the TES. Conversely, the thermal energy storage is discharged to produce electricity when the cost of electricity is higher or renewable energy generation is unavailable. The present study considers three distinct types of TES, as shown in Figure 2. The first TES adopted is a two-tank molten salt energy storage (M) with a temperature range of 295 to 580 °C (Turchi et al., 2019). During the charging phase, the cold molten salts flow into the EH and are then stored directly in the hot tank. During the discharge phase, the hot molten salts flow into the primary heater and provide the thermal power to operate the power block. Next, a two-silos setup that employs particles (P) as a storage medium is examined, with a maximum temperature of up to 1200 °C (Ma, 2020). The cold particles that are stored in the cold silo are conveyed via conveyor belts and allowed to free-fall into a direct particle EH. The third storage configuration is characterized by an air-packed bed (A), which can operate at temperatures higher than 1200 °C. During the charging phase of this system, air is passed through an EH and then into the packed bed, where thermal energy is stored in the rocks that serve as the storage medium. This is reversed during the discharge phase. 752

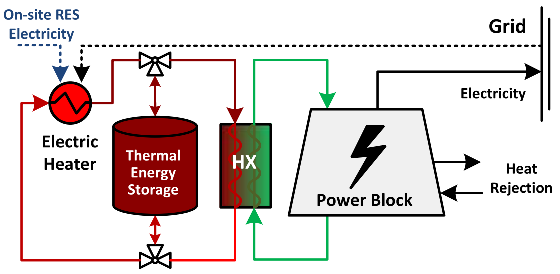


**Figure 1:** Layout of the energy storage plant

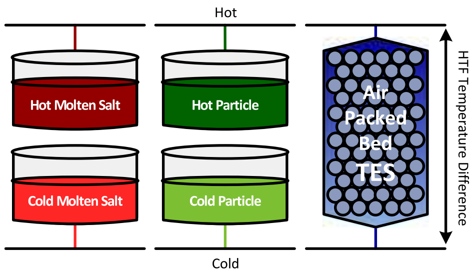


**Figure 2:** Thermal energy storage layouts

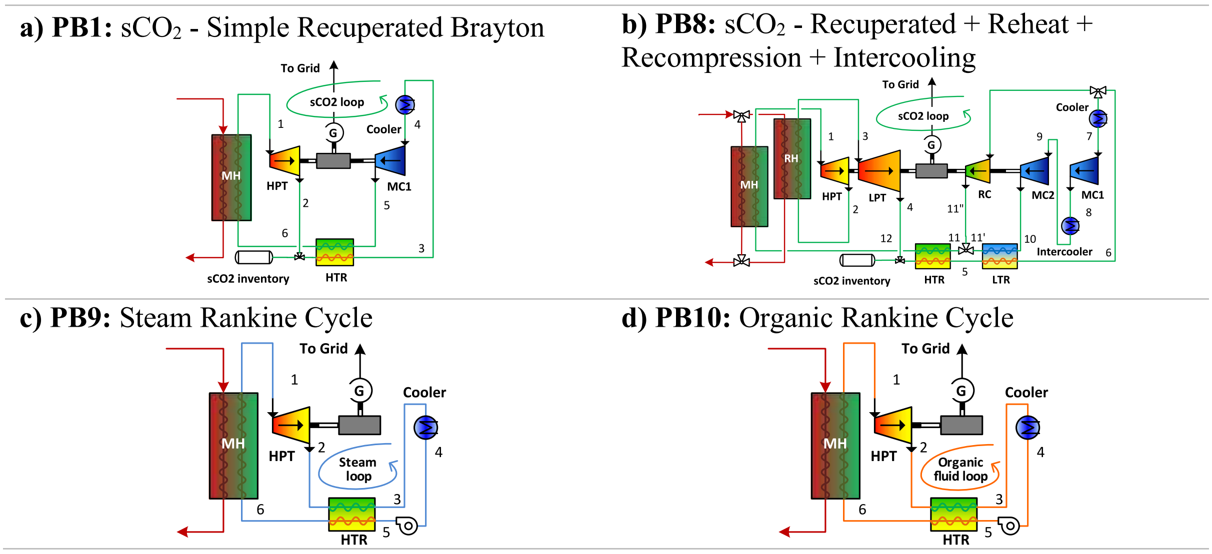


**Figure 3:** Power block configurations investigated

**Table 1:** Power block type description

| | | | |
|---|---|---|---|
| **PB1** | Simple Recuperated sCO2 Brayton | **PB2** | PB1 + Intercooling |
| **PB3** | PB1 + Reheat | **PB4** | PB3 + Intercooling |
| **PB5** | PB1 + Recompression | **PB6** | PB5 + Intercooling |
| **PB7** | PB1 + Reheat + Recompression | **PB8** | PB7 + Intercooling |
| **PB9** | Steam Rankine | **PB10** | Organic Rankine Cycle |

The analysis explores all potential combinations of these energy storage types and 10 power block configurations, while considering temperature limits and other boundary conditions. Figure 3 illustrates the power block layouts explored in this study, while Table 1 provides a description of each configuration to enhance clarity. These power blocks are labeled from 1 to 8 for the $sCO_2$-based layouts, 753
9 and 10 for the steam Rankine cycle and the organic Rankine cycle respectively. The eight $sCO_2$ power cycles have been outlined by modifying the simple recuperated Brayton cycle by employing intercooling, reheating, and recompression. All eight configurations are designed with dry cooling and feature turbomachinery on a single shaft, with variable speed gearboxes allowing for operation at different rotational speeds. Figure 3a and Figure 3b show the simplest and most efficient configurations of these layouts. Figure 3c shows the schematic of a recuperated steam Rankine cycle (PB9), while Figure 3d displays a recuperated organic Rankine cycle (PB10). The selection of organic fluids in the ORC cycle depends on the temperature of the heat source. Five distinct fluids have been utilized for this purpose. Isopentane has been employed for heat sources below 275 °C, while pentane is suitable for temperatures up to 325 °C. Cyclo-pentane is selected for temperatures ranging from 325 to 450 °C. Benzene, on the other hand, is considered for higher temperatures, up to 600 °C. The temperature ranges for these different organic fluids have been chosen to align with the limitations of the media and to optimize the thermal cycle efficiency within those ranges (Astolfi et al., 2018).

## 3 METHODOLOGY

The plant's techno-economic performance was evaluated using MoSES (Modeling of Solar Energy Systems), a Python-based tool developed by KTH Royal Institute of Technology. To evaluate the techno-economic indicators, the thermo-economics were coupled with an economic model based on a bottom-up estimation method, as shown in Figure 4. The thermodynamic states of the different media investigated in this study are estimated using CoolProp (Bell et al., 2014) The optimization problem was formulated to minimize the LCOS of the plant, an indicator to assess the relative profitability of the plant. The decision variables for the problem comprise of the thermal energy storage technology options including molten salt (M), particle (P), and air packed bed (A), power block layout, hot HTF temperature, and temperature difference between the hot and cold HTF temperatures in the TES.

$$LCOS = (CAPEX \cdot CRF + OPEX)/AEY \quad (1)$$

$$CRF = r \cdot (1 + r)^N/((1 + r)^N - 1) \quad (2)$$

The LCOS is a function of the investment cost (CAPEX), operational cost (OPEX), and Annual Energy Yield (AEY), as defined in equation (1). The Capital Recovery Factor (CRF), defined in equation (2), is a function of the lifetime ($N$), and the real discount rate ($r$).
The plant's operation assumes perfect daily charging and discharging cycles, as well as a constant electricity price. To begin, the energy storage plant is optimized for a capacity of 100 MWe and 12 hours of thermal energy storage, using a charging cost of 50 EUR/MWh, consistent with the average European spot price for the period 2020-2021 (European Network for Transmission System Operators in Electricity, 2023). A map is presented that outlines power block layouts and TES technologies, which minimize the LCOS for different HTF hot temperatures and temperature differences. Next, this study evaluates the impact of charging costs on system optimization and the best selections map by considering electricity costs of 0 and 100 EUR/MWh. The upper bound is selected based on the peaks of the average European spot prices (European Network for Transmission System Operators in Electricity, 2023), whereas the lower bound is used to simulate scenarios where surplus electricity is obtained from either the grid or on-site renewable generators. In the end, the effect of the scale has been investigated adopting capacities of 10 and 200 MWe.

### 3.1 Thermodynamic model

The amount of energy stored in the thermal energy storage technologies was determined as the product between the hours of storage ($TES_h$) and the thermal power design of the power block. The energy storage efficiency ($\eta_{TES}$) is determined by calculating the ratio of the energy discharged to the energy charged in a full storage cycle and is used to oversize the storage unit by accounting for thermal losses. For the commercial molten salt technology used in this study, an efficiency of 0.97 has been assumed for all combinations of HTF hot temperatures and hot-cold temperature differences (Turchi et al., 2019). In the case of the air packed bed layout, the TES efficiency ranges between 0.83 and 0.9, adopting a model developed by the authors in (Trevisan et al., 2020), which has been scaled with temperatures and validated in (Trevisan et al., 2022). The same approach has been implemented for the particle system, with efficiencies ranging between 0.87 and 0.94. Instead, the electric heater component was modeled using a fixed electric-to-thermal efficiency approach with an assumed efficiency of 0.95 for all the 754
different thermal energy storage technologies. The power block models were implemented by developing and interconnecting thermodynamic models of the main components, with media properties estimated trough integration of CoolProp into the model. The performance of the $sCO_2$ power cycles have been estimated following the methodology introduced by the authors in (Guccione et al., 2022), including the key assumptions and the correlations to consider the effect of size on isentropic efficiencies. A regression model was developed based on (Hirsch & Khenissi, 2014) to estimate the performance of the Rankine cycle at varying operating temperatures, pressures, and installed capacities. Similarly, a regression model was developed also for the ORC, based on (Astolfi et al., 2018), to estimate varying efficiencies based on the heat source temperature and the specific organic fluid used. Figure 5 displays the maximum temperature boundaries for the storage and power block layouts. The study calculates the return temperature for each power block layout, taking into account thermodynamic assumptions and cycle configurations. Consequently, more efficient $sCO_2$ cycle layouts are distinguished by higher return temperatures compared to the simple recuperated cycle, as an example.

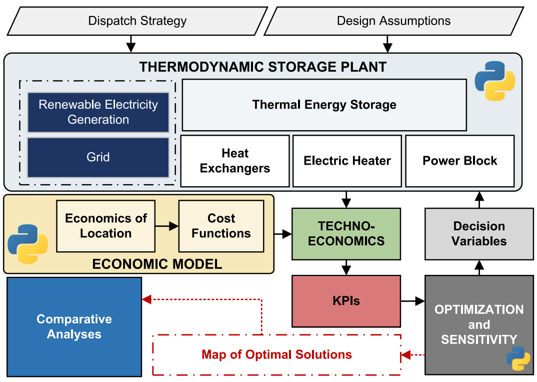


**Figure 4:** Methodology flowchart

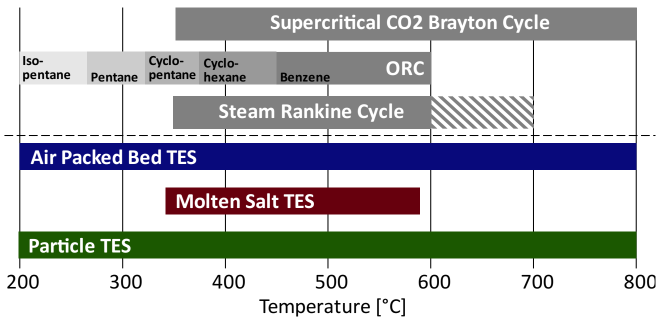


**Figure 5:** Maximum temperature limits

### 3.2 Economic model

The economic analysis of the storage plant takes into account two primary indicators, namely capital investment cost (CAPEX) and operational cost (OPEX). The capital investment includes both direct and indirect costs of all the main components involved in the storage plant as shown in equation (3). The operational cost comprises the charging cost and the operation and maintenance expenses of the plant, categorized as production-dependent and capacity-dependent yearly costs, as in equation (4). Table 2, provides a summary of the cost assumptions made for the plant's primary components. The main cost function developed by the authors are included in Appendix. A plant operational lifetime of 30 years was considered for the plant (USA DoE, 2019). The cost assumptions were converted into EUR based on the 2021 average USD-to-EUR exchange rate of 0.84 (European Central Bank, 2021). A nominal discount rate of 7% and an interest rate of 2.5% were adopted (USA DoE, 2019).

$$CAPEX = (C_{\text{site}} + C_{\text{TES}} + C_{\text{BOP}} + C_{\text{EH}} + C_{\text{PB}}) \cdot (1 + f_{\text{CONT}}) \cdot (1 + f_{\text{EPC}}) + C_{\text{land}} \tag{3}$$

$$OPEX = c_{\text{OM,fix}} \cdot P_{\text{net}} + c_{\text{OM,prod}} \cdot AEY + c_{\text{el}} \cdot E_{\text{charging}} \tag{4}$$

**Table 2:** Cost assumptions for the plant.

| Description | Unit | Value | Ref. |
|---|---|---|---|
| Electric heater (electrical) | EUR/kW | 15 | * |
| Electric heater (thermal) | EUR/kW | 125 | * |
| Temperature factor 1 | 1/°C | 16 | * |
| Temperature factor 2 | - | 0.2 | * |
| **Molten Salt** | | | |
| Storage | EUR/kWh$_t$ | 18–23 | (Turchi et al., 2019) - (Herrmann et al., 2004) |
| **Particle** | | | |
| Particle lift | EUR/(m-kg/s) | 49 | (González-portillo et al., 2021) |
| Particle silo | EUR/m$^2$ | 1033 | (González-portillo et al., 2021) |
| Particle | EUR/kg | 0.84 | (González-portillo et al., 2021) |
| **Air** | | | |
| High-T insulation | EUR/m$^3$ | 4303 | (Trevisan et al., 2020) |
| Low-T insulation | EUR/m$^3$ | 621 | (Trevisan et al., 2020) |
| Tank material | EUR/m$^3$ | 42693 | (Trevisan et al., 2020) |
| Rocks | EUR/m$^3$ | 67 | (Trevisan et al., 2020) |
| Foundations | EUR/m$^2$ | 1220 | (Trevisan et al., 2020) |
| **$sCO_2$ Power Block** | | | |
| Heater(s) | EUR/(W/K)$^{0.8778}$ | 14.7 | (Ho et al., 2015) |
| $sCO_2$ turbine | kEUR/(MW)$^{0.5561}$ | 15 | (Weiland et al., 2019) |
| $sCO_2$ compressor | kEUR/(MW)$^{0.3992}$ | 1033 | (Weiland et al., 2019) |
| $sCO_2$-$sCO_2$ recuperator | EUR/(W/K)$^{0.7544}$ | 41.5 | (Weiland et al., 2019) |
| $sCO_2$-Air cooler | EUR/(W/K)$^{0.75}$ | 27.6 | (Weiland et al., 2019) |
| Gearbox | kEUR/(MW)$^{0.2434}$ | 149 | (Weiland et al., 2019) |
| Generator | kEUR/(MW)$^{0.5463}$ | 92 | (Weiland et al., 2019) |
| $sCO_2$ piping | %PB cost | 15 (20) | (Weiland et al., 2019) |
| **Rankine Cycle** | | | |
| Steam specific cost | EUR/kW | 874 | (Turchi et al., 2019) |
| ORC specific cost | EUR/kW | 1000 | (Lemmens, 2015) |
| Reference size | kW | 100000 | (Turchi et al., 2019) |
| Scaling exponent | - | 0.7 | - |
| **Other costs** | | | |
| Land | EUR/m$^2$ | 2.1 | (Turchi et al., 2019) |
| Site Improvement | EUR/m$^2$ | 8.4 | (Turchi et al., 2019) |
| Balance of Plant | EUR/kW$_e$ | 244 | (Turchi et al., 2019) |
| Contingency | %direct costs | 7 | (Turchi et al., 2019) |
| EPC | %direct costs | 13 | (Turchi et al., 2019) |
| Fixed O&M cost – cap | EUR/kW-yr | 34 | (Turchi et al., 2019) |
| Variable O&M cost – gen | EUR/MWh-yr | 3 | (Turchi et al., 2019) |

*based on a real quotation

755

## 4 RESULTS AND DISCUSSION

Figure 6a shows the map of the TES configurations that minimize the LCOS of the plant considering different HTF hot temperature and temperature difference across the storage. Figure 6b illustrates the corresponding LCOS values associated with various combinations of temperatures, storage, and power block layouts. The changes in LCOS values are depicted through the marked contours, aligning with the colors shown in the color bar. To facilitate comparison, the identical color bar has also been employed for Figure 7b and Figure 7e. Figure 6c depicts the map of optimal power block layouts.

For a 100 MWe plant, the optimal LCOS with 12 hours of storage and an electricity cost of 50 EUR/MWh is achieved by coupling a particle TES with a $sCO_2$ power block with recompression and intercooling (PB6). The minimum LCOS value of 154.7 EUR/MWh is obtained at a HTF hot temperature ($T_{hot,HTF}$) of 750 °C and a design temperature difference ($\Delta T_{HTF}$) of 200 °C, as marked in Figure 6b. On one hand, reducing the temperature of the hot HTF can reduce costs for EH, TES, and power block, as it enables the use of less expensive materials. This also decreases the efficiency of converting thermal energy to electricity, resulting in higher LCOS. On the other hand, raising the HTF temperature can increase LCOS due to more expensive components, but also improve power block efficiency. Simultaneously, increasing the temperature difference across the TES can make storage more compact and cost-effective, but decrease storage efficiency. The power block layout and installed recuperator capacity determine the return temperature, and higher recuperation increases efficiency but also costs. Figure 6a shows that for most temperature combinations considered, the particle-based TES (P) offers the most cost-effective option. Although this TES has higher specific costs than an air-based TES, its higher efficiency leads to a lower electricity demand for charging compared to the air-based TES, resulting in a lower LCOS. The air-packed (A) TES is the optimal choice for regions characterized by low HTF temperatures and low temperature differences. At low HTF temperatures, the power block and electric heater costs become less significant, and the storage becomes the largest share of capital cost. Similarly, when the temperature difference decreases, the storage cost increases, making air-packed the optimal solution due to its lowest specific cost. The third region identified in Figure 6a is the molten salt TES (M), which is the best option when the design temperatures align with the limitations of the molten salt. The higher TES efficiency results in a significant reduction of charging power, leading to the lowest LCOS despite its higher specific costs compared to air and particle-based solutions. Figure 6c shows the optimal power block layouts for various design temperatures. The region of minimum LCOS is primarily occupied by $sCO_2$ power blocks with recompression and intercooling (PB6), along with a few configurations with recompression only (PB5). For temperature differences higher than 275 °C, simpler cycles such as $sCO_2$ simple recuperated (PB1) or simple recuperated with intercooling (PB2) with lower $sCO_2$ return temperatures should be preferred. The most complicated $sCO_2$ power block (PB8) is optimal only for low temperature differences and limited hot HTF temperatures, owing to its high efficiency and high return temperature.

In the region of low temperatures (up to 350 °C) and high temperature differences, the organic Rankine cycles (PB10) are the predominant choice. On the other hand, the steam Rankine cycle (PB9) is considered the optimal cycle between the low-temperature region and the region where the $sCO_2$ cycle is preferred. For high-temperature difference steam Rankine cycle is preferred to the $sCO_2$ one until the maximum hot temperature bounds for this technology is reached.

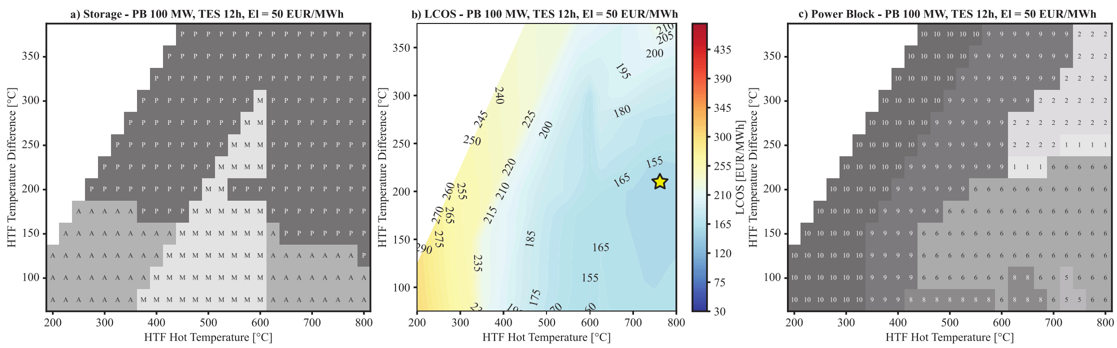


**Figure 6:** Map of optimal storage and power block layouts as a function of the design temperature across the thermal energy storage ($P_{PB}$ = 100 MW, $TES_h$ = 12 h, $c_{el}$ = 50 EUR/MWh)

756

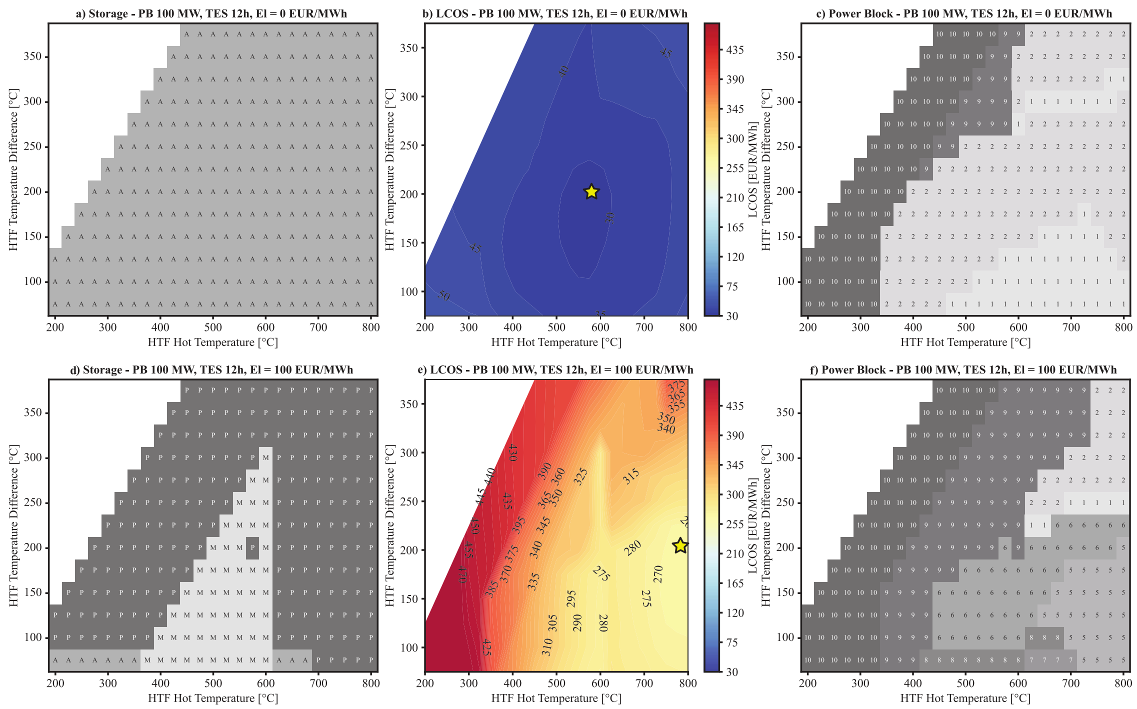


**Figure 7:** Sensitivity analysis on charging cost ($c_{el}$ = 0 and 100 EUR/MWh) - Maps of optimal storage and power block layouts ($P_{PB}$ = 100 MW, $TES_h$ = 12 h)

### 4.1 Sensitivity on installed capacity cost

A smaller scale system with a capacity of 10 MW yields a worse LCOS compared to the base-case, due to the lack of economy of scale. The highest HTF temperatures result in a minimum LCOS of 170 EUR/MWh. All optimal designs feature $sCO_2$ power blocks, which are compact and cost-efficient even at a small scale, unlike steam Rankine cycles. As the scale increases to 200 MW, the LCOS slightly decreases for all possible combinations of temperatures, storage, and power blocks. The storage selection remains relatively consistent with the base-case, while the power block map features more steam Rankine (PB9) configurations. At 200 MW, the minimum LCOS is achieved using a molten salt TES and a conventional steam Rankine cycle with maximum operating temperatures of 580 °C.



### 4.2 Sensitivity on charging cost

The cost breakdown of the LCOS showed that the charging cost is the most significant parameter affecting the maps proposed. Figure 7 presents the sensitivity on the optimal design maps for two charging cost scenarios: 0 and 100 EUR/MWh. In the first case, the optimal configuration is characterized by an air-packed bed TES coupled with a $sCO_2$ simple recuperated cycle with intercooling (PB2). A minimum LCOS of 30 EUR/MWh was achieved with a hot HTF temperature of 575 °C and a design temperature difference of 200 °C. When the electricity cost is zero, the optimal configuration is characterized by a less expensive TES and $sCO_2$ power block layout compared to the base-case analysis. Figure 7a indicates that air-packed bed TES is the most suitable option for most temperature combinations when the charging cost is negligible. Air-packed bed solutions are favorable in this scenario because the compressor power required to move air in the system has no impact on system cost. However, molten salt technology may be preferred due to its higher maturity when the temperatures are feasible, as the difference in performance between air and molten salt is less than 10%. Regarding power block selection, investing in more efficient power block cycles does not pay off, and a simple $sCO_2$ recuperated cycle or a simple cycle with intercooling is recommended.

Figure 7d, 7e, and 7f demonstrate that increasing the charging cost results in an increase in the minimum LCOS to 275 EUR/MWh, which is achieved with a hot temperature of 800 °C and a temperature difference of 200 °C. The optimal power block consists of an $sCO_2$ power block with recompression or recompression and intercooler (PB5, PB6) coupled with particle-based TES. The trend of optimal TES and power block layouts is like the base-case study, with a smaller region characterized by air-based TES. The $sCO_2$ power block layouts cover a larger region of the optimal selection map due to their lower costs and higher efficiencies. As the charging cost increases, the gap between the LCOS observed in the region where ORC layouts with low efficiency (23-30%) are utilized and the area where $sCO_2$ layouts are employed becomes even wider. Similarly to the base case, the ORCs are selected for the low-temperature region. One of the limitations of these findings is the assumption of a perfect daily cycling pattern with a fixed charging price, which may not reflect the real-world scenario. The optimal dispatch strategy would be influenced by the fluctuations in the charging cost. If there is a seasonal variation in charging cost, this will have a greater impact on the cost. A system like this would be more beneficial for a location with large daily changes in electricity prices.

## 5 CONCLUSIONS

This work introduced a techno-economic analysis to identify the best pairing of power cycle and thermal energy storage for a wide range of operating temperatures (200-800 °C). Various power block configurations are evaluated and coupled with different types of storage, including molten salt, particle, and air packed bed TES. To identify the most cost-effective combination of power cycle and TES, the study conducted an optimization aimed at minimizing the LCOS of the plant, considering different plant capacities and charging costs. Based on the results presented, the following conclusions can be drawn:

- The most cost-effective solution for a 100 MWe plant with 12 hours of storage and a charging cost of 50 EUR/MWh is the coupling of a $sCO_2$ power block with recompression and intercooling with a particle TES. The minimum LCOS value of 154.7 EUR/MWh was achieved with a temperature of 750 °C and a design temperature difference of 200 °C.
- When electricity is free, an intercooled $sCO_2$ power block coupled with an air-packed bed TES represents the most cost effective solution. An LCOS of 30 EUR/MWh can be achieved with a maximum HTF temperature of 575 °C. Air-packed bed TES should be preferred when storage represents a significant portion of the capital cost, especially with low HTF temperatures, low temperature differences, or low charging costs.
- A particle-based energy storage is the most cost-effective selection of TES for the largest region of the temperature combinations investigated, both at small (10 MW) and at larger scales (>100 MW).
- Molten salt is the suggested option for TES as long as the design temperatures fall within the temperature limitations of the salt, which are between 290 and 580 °C.



## NOMENCLATURE

| | | | |
|---|---|---|---|
| A | Air | MC (RC) | Main (Re-) Compressor |
| AEY | Annual Energy Yield | MH | Main Heater |
| BOP | Balance of Plant | OM | Operation and Maintenance |
| CAPEX | Capital Expenditure | OPEX | Operational Expenditure |
| CONT | Contingencies | ORC | Organic Rankine Cycle |
| EH | Electric Heater | P | Particle |
| EPC | Engineering, Procurement, Construction | PB | Power Block |
| H(L)PT | High (Low) Pressure Turbine | R | Reheat |
| HTF | Heat Transfer Fluid | RH | Re-Heater |
| H(L)TR | High (Low) Temp. Recuperator | RR | Recompression and Reheat |
| LCOS | Levelized Cost of Storage | TES | Thermal Energy Storage |
| M | Molten Salts | TIT | Turbine Inlet Temperature |

## REFERENCES


Al-Azawii, M. M. S., Alhamdi, S. F. H., Braun, S., Hoffmann, J. F., Calvet, N., & Anderson, R. (2021). Experimental study on packed-bed thermal energy storage using recycled ceramic as filler materials. *Journal of Energy Storage*, *44*(PA), 103375. https://doi.org/10.1016/j.est.2021.103375

Albert, M., Ma, Z., Bao, H., & Roskilly, A. P. (2022). Operation and performance of Brayton Pumped Thermal Energy Storage with additional latent storage. *Applied Energy*, *312*(January), 118700. https://doi.org/10.1016/j.apenergy.2022.118700

Astolfi, M., Alfani, D., Lasala, S., & Macchi, E. (2018). Comparison between ORC and CO2 power systems for the exploitation of low-medium temperature heat sources. *Energy*, *161*, 1250–1261. https://doi.org/10.1016/j.energy.2018.07.099

Bell, I. H., Wronski, J., Quoilin, S., & Lemort, V. (2014). Pure and pseudo-pure fluid thermophysical property evaluation and the open-source thermophysical property library coolprop. *Industrial and Engineering Chemistry Research*, *53*(6), 2498–2508. https://doi.org/10.1021/ie4033999

Benato, A., & Stoppato, A. (2018). Pumped Thermal Electricity Storage: A technology overview. *Thermal Science and Engineering Progress*, *6*, 301–315. https://doi.org/10.1016/j.tsep.2018.01.017

D'Aguanno, B., Karthik, M., Grace, A. N., & Floris, A. (2018). Thermostatic properties of nitrate molten salts and their solar and eutectic mixtures. *Scientific Reports*, *8*(1), 1–15. https://doi.org/10.1038/s41598-018-28641-1

European Central Bank. (2021). *Euro foreign exchange reference rates: average 2021 US dollar excahnge rate*. https://www.ecb.europa.eu/ stats/ policy_and_exchange_rates/ euro_reference_exchange_rates/ html/ eurofxref-graph-usd.en.html

European Network for Transmission System Operators in Electricity. (2023). *ENTSO-E Transparency Platform*. https://transparency.entsoe.eu/

Frate, G. F., Ferrari, L., & Desideri, U. (2020). Multi-Criteria Economic Analysis of a Pumped Thermal Electricity Storage (PTES) With Thermal Integration. *Frontiers in Energy Research*, *8*(April). https://doi.org/10.3389/fenrg.2020.00053

Glatzmaier, G. (2011). Developing a Cost Model and Methodology to Estimate Capital Costs for Thermal Energy Storage. *Nrel/Tp-5500-53066*, *December*, 1–17.

González-portillo, L. F., Albrecht, K., & Ho, C. K. (2021). *Techno-Economic Optimization of CSP Plants with Free-Falling Particle Receivers*. https://doi.org/10.3390/e23010076

Guccione, S., Trevisan, S., Guedez, R., Laumert, B., Maccarini, S., & Traverso, A. (2022, June 13). Techno-Economic Optimization of a Hybrid PV-CSP Plant With Molten Salt Thermal Energy Storage and Supercritical CO2 Brayton Power Cycle. *Proceedings of the ASME Turbo Expo 2022: Turbomachinery Technical Conference and Exposition. Volume 4: Cycle Innovations; Cycle Innovations: Energy Storage.* https://doi.org/10.1115/GT2022-80376

Hänchen, M., Brückner, S., & Steinfeld, A. (2011). High-temperature thermal storage using a packed bed of rocks - Heat transfer analysis and experimental validation. *Applied Thermal Engineering*, *31*, 1798–1806. https://doi.org/10.1016/j.applthermaleng.2010.10.034



Herrmann, U., Kelly, B., & Price, H. (2004). Two-tank molten salt storage for parabolic trough solar power plants. *Energy*, *29*(5–6), 883–893. https://doi.org/10.1016/S0360-5442(03)00193-2

Hirsch, T., & Khenissi, A. (2014). A systematic comparison on power block efficiencies for CSP plants with direct steam generation. *Energy Procedia*, *49*, 1165–1176. https://doi.org/10.1016/j.egypro.2014.03.126

Ho, C. K., Carlson, M., Garg, P., & Kumar, P. (2015). Cost and Performance Tradeoffs of Alternative Solar-Driven s-CO2 Brayton Cycle Configurations. *ASME 2015 9th International Conference on Energy Sustainability Collocated with the ASME 2015 Power Conference*. https://doi.org/10.1115/ES2015-49467

Hu, S., Yang, Z., Li, J., & Duan, Y. (2021). Thermo-economic analysis of the pumped thermal energy storage with thermal integration in different application scenarios. *Energy Conversion and Management*, *236*, 114072. https://doi.org/10.1016/j.enconman.2021.114072

Laughlin, R. B. (2017). Pumped thermal grid storage with heat exchange. *Journal of Renewable and Sustainable Energy*, *9*(4). https://doi.org/10.1063/1.4994054

Lemmens, S. (2015). A Perspective on Costs and Cost Estimation. *Proceedings of the 3rd International Seminar on ORC Power Systems*, *2010*, 1–10.

Liang, T., Vecchi, A., Knobloch, K., Sciacovelli, A., Engelbrecht, K., Li, Y., & Ding, Y. (2022). Key components for Carnot Battery: Technology review, technical barriers and selection criteria. *Renewable and Sustainable Energy Reviews*, *163*(May), 112478. https://doi.org/10.1016/j.rser.2022.112478

Ma, Z. (2020). *Particle Thermal Energy Storage Components for Pumped Thermal Energy Storage*.

Morandin, M., Maréchal, F., Mercangöz, M., & Buchter, F. (2012). Conceptual design of a thermo-electrical energy storage system based on heat integration of thermodynamic cycles - Part A: Methodology and base case. *Energy*, *45*(1), 375–385. https://doi.org/10.1016/j.energy.2012.03.031

Trevisan, S., Guédez, R., & Laumert, B. (2020). Thermo-economic optimization of an air driven supercritical CO2 Brayton power cycle for concentrating solar power plant with packed bed thermal energy storage. *Solar Energy*, *211*(October), 1373–1391. https://doi.org/10.1016/j.solener.2020.10.069

Trevisan, S., Wang, W., Guedez, R., & Laumert, B. (2022). Experimental evaluation of a high-temperature radial-flow packed bed thermal energy storage under dynamic mass flow rate. *Journal of Energy Storage*, *54*. https://doi.org/https://doi.org/10.1016/j.est.2022.105236

Turchi, C. S., Boyd, M., Kesseli, D., Kurup, P., Mehos, M., Neises, T., Sharan, P., Wagner, M. J., & Wendelin, T. (2019). CSP Systems Analysis - Final Project. *Nrel/TP-5500-72856*, *May*.

USA DoE. (2019). *Gen 3 CSP Topic 1–Phase 3 Test Facility Down-Selection Criteria*.

Vecchi, A., Knobloch, K., Liang, T., Kildahl, H., Sciacovelli, A., Engelbrecht, K., Li, Y., & Ding, Y. (2022). Carnot Battery development: A review on system performance, applications and commercial state-of-the-art. *Journal of Energy Storage*, *55*(PD), 105782. https://doi.org/10.1016/j.est.2022.105782

Weiland, N. T., Lance, B. W., & Pidaparti, S. R. (2019). sCO2 Power Cycle Component Cost Correlations From DOE Data Spanning Multiple Scales and Applications. *ASME Turbo Expo 2019: Turbomachinery Technical Conference and Exposition*, *9*, 1–17. https://doi.org/10.1115/GT2019-90493

White, M. T., Bianchi, G., Chai, L., Tassou, S. A., & Sayma, A. I. (2021). Review of supercritical CO2 technologies and systems for power generation. *Applied Thermal Engineering*, *185*(December 2020). https://doi.org/10.1016/j.applthermaleng.2020.116447

## ACKNOWLEDGEMENT

The authors acknowledge the financial support from the European Union's Horizon 2020 research and innovation program, project No. 952953.

## APPENDIX

*Electric Heater*

$$C_{\text{EH}} = c_{\text{EH}} \cdot P_{\text{EH,des}} \quad \text{(a)}$$

$$c_{\text{EH}} = c_{\text{EH,el}} + c_{\text{EH,th}} \cdot f_{\text{T,EH}} \quad \text{(b)}$$

$$f_{\text{T,EH}} = c_1 \cdot \log(T_{\max}\,[°C]) - c_2 \quad \text{(c)}$$

*Air Packed Bed TES*

$$C_{\text{TES}} = c_{\text{rocks}} \cdot V_{\text{rocks}} + \left( c_{\text{HT}_{\text{ins}}} \cdot V_{\text{HT}_{\text{ins}}} + c_{\text{LT}_{\text{ins}}} \cdot V_{\text{LT}_{\text{ins}}} + c_{\text{mat}} \cdot V_{\text{mat}} \right) \cdot fT_{\text{TES}} + c_{\text{foundations}} \cdot A_{\text{land}_{\text{TES}}} \quad \text{(d)}$$

*Molten Salt TES*

$$C_{\text{TES}} = c_{\text{TES}} \cdot E_{\text{TES,des}}{}^{*} \quad \text{(e)}$$

*The specific molten salt TES cost model is calculated using the following approach:

$$c_{\text{TES}} = c_{\text{media,TES}} / (1 - \%_{\text{non-media}}) \quad \text{(f)}$$

where $c_{media,TES}$ is the TES specific cost proportional to the medium and $\%_{nonmedia}$ is the complementary share of the TES cost. The specific TES cost ($c_{TES,1}$) has been assumed equal to 23 EUR/kWh for a TES temperature difference between the hot and cold tank ($\Delta T_{TES,1}$) equal to 98 °C (Turchi et al., 2019). For $\Delta T_{TES,1}$, the share of non-media TES can be assumed equal to 0.55 (Turchi et al., 2019). Similarly, for $\Delta T_{TES,2}$ equal to 275 °C, the share of non-media TES can be assumed equal to 0.54 (Glatzmaier, 2011) and the specific cost $c_{TES,2}$ can be assumed equal to 18 EUR/kWh (Turchi et al., 2019). Then, for a given $\Delta T_{TES}$, the $c_{media,TES}$ is calculated as in equation (g). The parameters $a1_{TES}$ is defined in equation (h). The share of non-media is estimated as a function of the $\Delta T_{TES}$ as in equation (i), where the parameters $a2_{TES}$ is calculated as in equation (j).

$$c_{\text{media,TES}} = a1_{\text{TES}} \cdot \Delta T_{\text{TES}} + \left(c_{\text{media,TES,1}} - \Delta T_{\text{TES,1}} \cdot a1_{\text{TES}}\right) \quad \text{(g)}$$

$$a1_{\text{TES}} = \frac{c_{\text{media,TES,2}} - c_{\text{media,TES,1}}}{\Delta T_{\text{TES,2}} - \Delta T_{\text{TES,1}}} \quad \text{(h)}$$

$$\%_{\text{non-media}} = a2_{\text{TES}} \cdot \Delta T_{\text{TES}} + \left(\%_{\text{nonmedia,1}} - \Delta T_{\text{TES,1}} \cdot a1_{\text{TES}}\right) \quad \text{(i)}$$

$$a2_{\text{TES}} = \frac{\%_{\text{non-media,2}} - \%_{\text{non-media,1}}}{\Delta T_{\text{TES,2}} - \Delta T_{\text{TES,1}}} \quad \text{(j)}$$

**If reheat is included in the power block, the share of piping cost is equal to 0.2, otherwise 0.15.

This book contains the compilation of works contributed to the *7th International Seminar on Organic Rankine Cycle Power Systems* (ORC 2023), held in Seville between the 4th and 6th of September 2023. The event was hosted by Universidad de Sevilla on behalf of the Knowledge Centre on Organic Rankine Cycle Technology (KCORC), incorporated in The Netherlands.

The ORC conference, organized biennially, stems as the only conference that is specific to ORC technology, therefore gathering a diverse community whose affiliation spans across all the interested stakeholders, not only in this particular technology but also and in a broader context, in the energy transition. Original equipment manufacturers, professional associations, end-users, investors, policy makers, academics, scientists feel at home at ORC 2023.

The almost 100 proceedings in this book cover a wide variety of topics, from fundamentals to system integration through component design, accounting for thermodynamic performance as well as component design. In addition to this, and as a new track in 2023, works on heat pump technology were also accepted in order to raise awareness of the strong ties between both technologies, specifically in energy storage applications.

This book provides an excellent overview of the current maturity of power systems based on Organic Rankine Cycle technology for applications as diverse as geothermal and waste heat recovery in industry or downstream of other prime movers (e.g., marine applications). It is also an excellent source of information to understand the current challenges faced by the technology, stemming from a very competitive market and increasingly stringent environmental regulations.

The organizers of ORC 2023 hope that the reader finds this work as exciting as the attendees to the conference and, maybe, make the decision to join the 8th edition to the conference in 2025.

KCORC
KNOWLEDGE CENTER
ORGANIC RANKINE CYCLE

eus EDITORIAL
UNIVERSIDAD DE SEVILLA